Optimal model-free backstepping control for a quadrotor helicopter

Hossam Eddine Glida, Latifa Abdou, Abdelghani Chelihi, Chouki Sentouh, Seif-El-Islam Hasseni

Nonlinear Dynamics 100/4 (2020) 3449-3468

Optimal model-free backstepping control for a quadrotor helicopter

Hossam Eddine Glida · Latifa Abdou · Abdelghani Chelihi · Chouki Sentouh · Seif-El-Islam Hasseni

Abstract This paper proposes a design of a direct optimal control for a class of multi-input–multi-output (MIMO) nonlinear systems. This work focuses on the design of optimal model-free backstepping controller for a MIMO quadrotor helicopter perturbed by unknown external disturbances. The proposed method consists of using a model-free-based backstepping controller optimized by a cuckoo search algorithm. First, the overall dynamic model is decoupled into six interconnected subsystems. Then, the ideal backstepping controller with a known dynamic function is designed for each subsystem. The model-free based on backstepping control uses a new estimator approach to approximate the unknown dynamic model functions. After that, the global asymptotical stability of the closed-loop control system is proved via the Lyapunov theory. Moreover, the parameters of the proposed controller are optimized by the cuckoo search algorithm according to a cost function. The results of numerical simulations applied to the quadrotor helicopter system demonstrate the robustness and the effectiveness of the proposed control strategy.

Keywords Quadrotor helicopter · Model-free control · Backstepping controller · Optimization · Cuckoo search algorithm

H. E. Glida (✉) · S.-E.-I. Hasseni
LMSE Laboratory, Department of Electrical Engineering, University of Biskra, Biskra, Algeria
e-mail: hossam.gld@hotmail.com

S.-E.-I. Hasseni
e-mail: seif.hasseni@univ-biskra.dz

L. Abdou · A. Chelihi
LI3CUB Laboratory, Department of Electrical Engineering, University of Biskra, Biskra, Algeria
e-mail: abdou@univ-biskra.dz

A. Chelihi
Department of Electronics, Faculty of Technology, Constantine 1 University, Constantine, Algeria
e-mail: chelihi.abdelghani@yahoo.fr

C. Sentouh
LAMIH-UMR CNRS 8201, Department of Automatic Control, Hauts-de-France Polytechnic University, Valenciennes, France
e-mail: Chouki.Sentouh@uphf.fr

1 Introduction

In the recent decade, the quadrotor unmanned aerial vehicles (UAVs) have received much attention in various applications due to their high performance, mechanical simplicity, high maneuver ability and their several application purposes in civil and military areas such as agriculture domain, monitoring and supervision [31,41]. In fact, the quadrotor UAVs tracking control is an open search problem. This type of aerial vehicle is an open-loop unstable system, which requires a high response controller and large control domain. Also, they are characterized by the nonlinearities and the underactuated property which lead to strong coupling between their state variables. See even more, these devices are very sensitive systems to external dis-

DOI : 10.1007/s11071-020-05671-x

turbances such as wind effect, friction and the uncertainties [47].

1.1 Related works on quadrotor control

The quadrotor UAV can be considered as a large-scale multi-input–multi-output (MIMO) system with six degrees of freedom (DOFs), and its mathematical model is characterized by its nonlinearity and complexity. Obviously, it is difficult to achieve an appropriate control for this system by using classical linear control laws such as proportional–integral–derivative controller (PID) [4] and linear quadratic regulator (LQR) [33], due to the fact that the quadrotor is an underactuated system and its model is characterized by its strong interconnected functions. There are several researches and developments on the quadrotor UAVs and many nonlinear control approaches that have been proposed [1,14,15,30,32,44]. Feedback linearization is widely used for an unmanned quadrotor helicopter control [32]. In [1], authors proposed many control laws for testing the performance of an unmanned quadrotor helicopter, sliding-mode control, backstepping control, feedback linearization-based control and fuzzy control schemes. An adaptive sliding-mode control law was proposed in [30] for the overall UAV system control with uncertain parameters without knowledge of the upper bound on the system uncertainty in advance. A disturbance observer-based sliding-mode control scheme was proposed in [44]. Hybrid strategy for integral backstepping sliding-mode control under an external uncertain disturbances was proposed in [14]. Also, a backstepping non-singular terminal sliding-mode control with an adaptive algorithm applied to a quadrotor with an adaptive tuning method was used to deal with the external disturbances [15].

The model-free control (MFC) theory that was introduced in several works as in [8,9] and therein references, it is applied to the quadrotor UAV in few modest papers [2,6,20]. In [2,6], a robust MFC has been used to ensure the robustness and the stability of the control system. The proposed MFC laws in these papers are based on the feedback linearization technique which showed satisfactory results when they are applied to a small quadrotor. Model-free control using adaptive proportional-derivative sliding-mode control with robust integral of the signum of the error was developed for quadrotor helicopter in [20]. However, the control systems developed in these studies are based on the known local model that must be defined in short operating time. Consequently, the stability is proven only locally and nothing can be said about overall (global) stability of closed-loop system. In the present work, the proof of global stability based on Lyapunov theory is made on the overall quadrotor system. In addition, the design parameters in the aforementioned MFC schemes are selected by the user via the trial-and-error method during simulation tests. So, it seems incapable of finding any specific criteria to guarantee the optimal behavior of the proposed control laws.

1.2 Proposed methodology

Motivated by the above literature, we propose in this study an optimal model-free backstepping control (OMFBC) law applied to a quadrotor UAV, including the rotation and position motion of the body. The objective of this control strategy is to track a desired trajectory of a 6DOF quadrotor position and attitude with unknown nonlinear dynamics and external disturbances. Here, the quadrotor UAV is considered as MIMO large-scale system and can be decomposed into six interconnected single-input–single-output (SISO) subsystems that describe one DOF, i.e., three-angle subsystems and three position subsystems. Then, for each subsystem, a control law is developed based on a combination of optimized backstepping technique and the adaptive nonlinear estimator. The design parameters of our control strategy are tuned by using metaheuristic algorithm when the estimators are employed to deal with the unknown nonlinear dynamics and external disturbances. The global stability of quadrotor UAV system in trajectory tracking control problem is demonstrated by Lyapunov method.

Several successful works based on metaheuristic algorithms proved their convergence to the optimal solution for optimization problems, such as genetic algorithms (GA) used in [13] to tune the parameters of a PID décentralized controller applied to a quadrotor. Also, a GA is proposed to solve combinatorial optimization problem for scheduling the aerial recovery of multiple unmanned aerial vehicles in [23]. The parameters of a backstepping controller for a dynamic model of nominal helicopter were optimized via particle swarm optimization (PSO) in [27]. The PSO was proposed in [7] as an improved stochastic variant strategy to tune

the gains of the fuzzy PID controller, a recent research used the PSO algorithm to tune the parameters of a model-free based on PID controller for vibration control of an active vehicle suspension systems [29], and PSO was used to determine the parameters of database controller for active suspension control [36]. A phase angle-encoded fruit fly optimization algorithm with mutation adaptation mechanism was proposed with a path planner by [46]. The recently developed metaheuristic swarm intelligent methods are widely used to solve the UAV path planning problems [40,48]. In this work, we propose to use the cuckoo search algorithm (CSA) to define the optimal parameters of the proposed controller. The CSA is one of the most effective optimization algorithms, which proved their effectiveness to resolve many works [18,45]. This technique is mainly characterized by its convergence speed to achieve the optimal solution in few generations.

1.3 Contributions

This paper investigates a new optimal controller design for the nonlinear quadrotor system. This approach claims the following elements:

1. The mathematical model of the quadrotor based on the Newton–Euler formalism is presented; then, based on the quadrotor physical architecture a state space model seen as large-scale system is given.
2. The development of a model-free backstepping controller that satisfies the overall closed-loop stability and compensates the unknown dynamics as well as the external disturbances.
3. In order to improve the tracking performances for quadrotor responses, an optimization of the controller parameters via cuckoo search metaheuristic algorithm is introduced.
4. The simulation tests are performed to that the designed controller is able to maintain best performance of the quadrotor UAV even in the presence of unknown dynamics and external disturbances.

Therefore, the proposed optimal model-free control approach leads to major advantages compared to existing works and its main contributions are important. The particular features of this model-free-based control solution can be summarized as follows:

- Compared with backstepping techniques [14,15,19,26,27], the SMC approaches [28,30,47] and the PID and LQR controllers [13,33], the proposed MFC has a strong robustness against unknown nonlinearities, parameter variations and external disturbances and keeps some characteristics of classical control techniques such as simplicity and continuous control signals. In addition, the control problem of MIMO nonlinear systems is solved by converting it to the easy SISO control synthesis which depends only on the real-time measurement data of quadrotor UAV.
- Unlike in references [2,20] where the authors presented a MFC taking into account that the quadrotor can be modeled by known local or partial model which considerably limits the range of their applicability in real time. In the present paper, a successful development of a new nonlinear model-free control law for quadrotor system that does not require any prior knowledge of its dynamic model is proposed. Moreover, the developed controller is designed with less restrictive conditions on the control gains and external disturbances which are assumed to be bounded unknown nonlinear functions.
- In [5,42], authors propose a complex MFC approaches based on adaptive intelligent networks to control quadrotor UAVs. In these controllers, neural networks and/or fuzzy systems are used to approximate the uncertainties of quadrotor model caused by unmodeled dynamics, parameters variations and external disturbances. However, the design parameters of these networks are selected randomly and require expert's knowledge. For these reasons, this paper investigates a simple adaptive nonlinear estimator to deal all unknown nonlinear functions of quadrotor model and the backstepping control technique to design a robust and straightforward model-free controller.
- In [2,12,33,43], the authors propose different control techniques for driving UAVs where the simulation results show a good trajectory tracking performance. However, the obtained results remain insufficient since the system stability of these control strategies is validated only locally which decrease the reliability of the controller. Instead, in the proposed work, the stability analysis and the convergence of the tracking errors of quadrotor subsystems as well as of the overall closed-loop system are guaranteed via the Lyapunov method arguments in all operating space. Moreover, the proposed MFC

deals the quadrotor model with dynamics and disturbances totally unknowns, while in [43], a partially uncertain quadrotor model case is considered.
- Unlike in [2,19,21] and numerous related references, the controller's parameters are selected generally by using the trial-and-error method leading in effect to great limitation of these approaches. Though, the best performances of control system are not achieved. Instead, in the present work, the optimal behavior of the proposed controller is ensured by tuning its parameters using a new metaheuristic algorithm called "the cuckoo search technique," whose effectiveness and merits are exemplified by conducting several simulation cases. This approach allows to provide a systematic procedure for tuning the control parameters and so to increase the performances of many application systems in different engineering fields such as spacecraft systems, electric drives, mechanical arms and many other systems in human life.

This paper is organized follows. Section 2 discusses the dynamic model of the quadrotor helicopter obtained via Euler–Newton formalism and used for simulation purposes. Section 3 describes the controller design process and the stability analysis of the conventional backstepping controller. The optimal model-free backstepping law based on cuckoo search algorithm is discussed in Sect. 4. The numerical results to demonstrate the effectiveness of the proposed controller are presented in Sect. 5. Finally, the conclusion of this study is elaborated in Sect. 6.

2 Rigid-body dynamics

The quadrotor is considered as one of the most complex UAVs dynamic considering its six-degree-of-freedom (6-DOF) nonlinearities (i.e., nonlinear system, strong coupling system and underactuated system), whose mathematical dynamic model is derived via Newton–Euler formalism. To understand its movement, we have to place two coordinates: The first is a static Galilei coordinate of the earth frame $E(x_\mathrm{e}, y_\mathrm{e}, z_\mathrm{e})$ and the other one is $B(x_\mathrm{b}, y_\mathrm{b}, z_\mathrm{b})$ body-fixed frame placed on the structure coincident to the vehicle inertia axes as shown in Fig. 1. The solid structure of the quadrotor is assumed to be symmetrical; also, the thrust and drag are proportional to the square of the propellers speed.

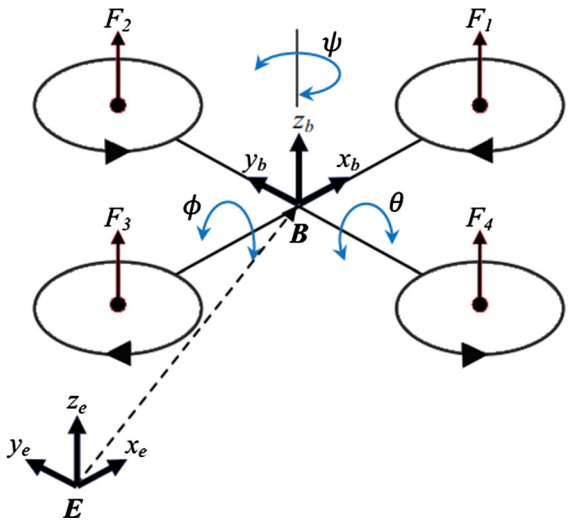

Fig. 1 Quadrotor configuration

2.1 System model

The position of the quadrotor in the earth frame is represented by $\wp = [x, y, z]^\mathrm{T}$ and $\xi = [\dot{x}\ \dot{y}\ \dot{z}]^\mathrm{T}$ is the translation velocity vector, where x, y and z denote the position of the quadrotor with respect to $E(x_\mathrm{e}, y_\mathrm{e}, z_\mathrm{e})$, $\Phi = [\phi\ \theta\ \psi]^\mathrm{T}$ is the attitude quadrotor vector and $\omega = [\dot{\phi}\ \dot{\theta}\ \dot{\psi}]^\mathrm{T}$ is the angular velocity vector, where ϕ, θ, ψ called the Euler angles (roll angle, pitch angle and yaw angle) in $E(x_\mathrm{e}, y_\mathrm{e}, z_\mathrm{e})$ and $\dot{\phi}, \dot{\theta}, \dot{\psi}$ are the angular velocity of roll, pitch and yaw with respect to $B(x_\mathrm{b}, y_\mathrm{b}, z_\mathrm{b})$. The dynamic equations of a quadrotor translational can be written via Newton–Euler formalism as follows:

$$m\dot{\xi} = -mg\varpi_z + u_1 R\varpi_z \tag{1}$$

where m is the mass of the quadrotor, g is the gravitational constant and $\varpi_z = [0, 0, 1]^\mathrm{T}$ is the unit vector expressed in the frame $E_{(x_\mathrm{e},y_\mathrm{e},z_\mathrm{e})}$. The transition from the fixed reference $E_{(x_\mathrm{e},y_\mathrm{e},z_\mathrm{e})}$ to the moving reference $B_{(x_\mathrm{b},y_\mathrm{b},z_\mathrm{b})}$ is done through homogeneous matrix transformation R as:

$$R = \begin{pmatrix} c\theta c\psi & c\psi s\theta c\phi - s\psi c\phi & c\psi s\theta c\phi + s\psi s\phi \\ c\theta s\psi & s\psi s\theta s\phi + c\psi c\phi & s\psi s\theta c\phi - c\psi s\phi \\ -s\theta & s\phi c\theta & c\phi c\theta \end{pmatrix} \tag{2}$$

where s and c denote sin(.) and cos(.), respectively.

The rotation of the four rotors produces a total thrust u_1 given as:

$$u_1 = \sum_{i=1}^{4} F_i = b \sum_{i=1}^{4} \Omega_i^2 \tag{3}$$

where F_i is the thrust force, Ω_i represents the angular speed of each rotor $i \in \{1, 2, 3, 4\}$ and b is the thrust factor. The dynamics equation of attitude motion can be derived from the Euler formulation as follows:

$$I\dot{\omega} = -\omega \times I\omega - \Gamma_g + \tau \tag{4}$$

where $I = diag[I_x, I_y, I_z] \in \Re^{3\times3}$ is the symmetric positive definite inertia matrix with respect to $B_{(xb,yb,zb)}$, Γ_g is the gyroscopic effect due to rigid body rotation, its expression is given by:

$$\Gamma_g = \sum_{i=1}^{4} \Omega_i \times J_r(\omega^{\mathrm{T}} \times \begin{pmatrix} 0 \\ 0 \\ 1 \end{pmatrix})(-1)^{i+1} \tag{5}$$

where J_r is the rotor inertia and τ is the control torque obtained by varying the rotor speeds:

$$\tau = \begin{pmatrix} lu_2 \\ lu_3 \\ u_4 \end{pmatrix} = \begin{pmatrix} -k_p\Omega_1^2 + k_p\Omega_3^2 \\ -k_p\Omega_2^2 + k_p\Omega_4^2 \\ k_d\Omega_1^2 - k_d\Omega_2^2 + k_d\Omega_3^2 - k_d\Omega_4^2 \end{pmatrix} \tag{6}$$

where l is the length between the quadrotor center of mass and the rotation axis of propeller, k_p is the thrust factor, k_d is the drag factor and u_2, u_3 and u_4 are the forces with respect to the x-, y- and z-axis of the body frame, respectively.

From (1) and (4), the mathematical dynamic model of the quadrotor in order to represent the evolution of position and rotation is written as:

$$\begin{aligned}
\ddot{x} &= \frac{c\psi s\theta c\phi + s\psi s\phi}{m} u_1 \\
\ddot{y} &= \frac{c\psi s\theta s\phi - c\psi c\phi}{m} u_1 \\
\ddot{z} &= \frac{c\phi c\theta}{m} u_1 - g \\
\ddot{\phi} &= \frac{I_y - I_z}{I_x}\dot{\theta}\dot{\psi} - \frac{J_r\Omega_r}{I_x}\dot{\theta} + \frac{l}{I_x}u_2 \\
\ddot{\theta} &= \frac{I_z - I_x}{I_y}\dot{\phi}\dot{\psi} + \frac{J_r\Omega_r}{I_y}\dot{\phi} + \frac{l}{I_y}u_3 \\
\ddot{\psi} &= \frac{I_x - I_y}{I_z}\dot{\phi}\dot{\psi} + \frac{1}{I_z}u_4
\end{aligned} \tag{7}$$

where

$$\Omega_r = \Omega_1 - \Omega_2 + \Omega_3 - \Omega_4. \tag{8}$$

Considering Eq. (7), six second-order differential equations are contained to constitute the quadrotor nonlinear model under the design conditions described in the literature [21]. The total and lift forces obtained by varying the rotor speeds in Eqs. (3) and (5) denoted as u_1, u_2, u_3 and u_4, respectively, are taken as the control inputs, namely $\mathcal{U} = [u_1\ u_2\ u_3\ u_4]^{\mathrm{T}}$. The position and the attitude of quadrotor denoted as $\wp$ and Φ, respectively, are set as the outputs, namely $y = [x, y, z, \phi, \theta, \psi]^{\mathrm{T}}$, see [27]. The dynamic Eq. (7) is considered as an affine nonlinear system which can be written in the following form:

$$\dot{\chi} = \mathcal{F}(\chi) + \mathcal{G}(\chi)\mathcal{U} \tag{9}$$

where $\chi \in \Re^{12}$ represents the state variables and $\mathcal{F}(\chi) \in \Re^{12\times1}$ and $\mathcal{G}(\chi) \in \Re^{12\times4}$ are nonlinear functions matrix, with:

$$\begin{aligned}
\chi &= [\chi_{x,1}, \chi_{x,2}, \chi_{y,1}, \chi_{y,2}, \chi_{z,1}, \chi_{z,2}, \chi_{\phi,1}, \\
&\quad \chi_{\phi,2}, \chi_{\theta,1}, \chi_{\theta,2}, \chi_{\psi,1}, \chi_{\psi,2}]^{\mathrm{T}} \\
&= [x, \dot{x}, y, \dot{y}, z, \dot{z}, \phi, \dot{\phi}, \theta, \dot{\theta}, \psi, \dot{\psi}]^{\mathrm{T}}
\end{aligned} \tag{10}$$

$$\mathcal{F}(\chi) = \begin{pmatrix} \chi_{x,2} \\ 0 \\ \chi_{y,2} \\ 0 \\ \chi_{z,2} \\ -g \\ \chi_{\phi,2} \\ \frac{I_y - I_z}{I_x}\chi_{\theta,2}\chi_{\psi,2} - \frac{J_r\Omega_r}{I_x}\chi_{\theta,2} \\ \chi_{\theta,2} \\ \frac{I_z - I_x}{I_y}\chi_{\phi,2}\chi_{\psi,2} + \frac{J_r\Omega_r}{I_y}\chi_{\phi,2} \\ \chi_{\psi,2} \\ \frac{I_x - I_y}{I_z}\chi_{\theta,2}\chi_{\phi,2} \end{pmatrix} \tag{11}$$

$$\mathcal{G}(\chi) = \begin{pmatrix} 0 & 0 & 0 & 0 \\ \frac{c\chi_{\phi,1}s\chi_{\theta,1}c\chi_{\psi,1} + s\chi_{\psi,1}s\chi_{\phi,1}}{m} & 0 & 0 & 0 \\ 0 & 0 & 0 & 0 \\ \frac{c\chi_{\phi,1}s\chi_{\theta,1}s\chi_{\psi,1} - s\chi_{\psi,1}c\chi_{\phi,1}}{m} & 0 & 0 & 0 \\ 0 & 0 & 0 & 0 \\ \frac{s\chi_{\phi,1}c\chi_{\theta,1}}{m} & 0 & 0 & 0 \\ 0 & 0 & 0 & 0 \\ 0 & \frac{l}{I_x} & 0 & 0 \\ 0 & 0 & 0 & 0 \\ 0 & 0 & \frac{l}{I_y} & 0 \\ 0 & 0 & 0 & 0 \\ 0 & 0 & 0 & \frac{1}{I_z}. \end{pmatrix} \tag{12}$$

Remark 1 It should be noted that the previous quadrotor model is obtained after some simplifications in its physical conception, such as the quadrotor has a rigid and symmetric body. The four rotors and propellers of the quadrotor have the same characteristics. The roll, the pitch and the yaw angles, ϕ, θ and ψ are bounded as $\frac{-\pi}{2} < \phi < \frac{\pi}{2}$, $\frac{-\pi}{2} < \theta < \frac{\pi}{2}$ and $-\pi < \phi < \pi$ [21].

2.2 Problem formulation

From representation (9), the quadrotor model can be considered as a large-scale MIMO system which is composed of six interconnected subsystems, i.e., each output is represented by a SISO nonlinear subsystem. However, since the quadrotor is an underactuated system in which the six outputs $y_i \in \{x, y, z, \phi, \theta, \psi\}$ are controlled only by four inputs $u_i \in \{u_1, u_2, u_3, u_4\}$, it is difficult to control all the six subsystems independently. To overcome this problem, two virtual control inputs u_x and u_y are created to drive the Cartesian position subsystems x and y, respectively [17,21]. From Eqs. (9) and (12), their expressions are chosen as follows:

$$u_x = (c\chi_{\phi,1} s\chi_{\theta,1} c\chi_{\psi,1} + s\chi_{\psi,1} s\chi_{\phi,1}) u_z \tag{13}$$

$$u_y = (c\chi_{\phi,1} s\chi_{\theta,1} s\chi_{\psi,1} - s\chi_{\psi,1} c\chi_{\phi,1}) u_z. \tag{14}$$

Then, let $\chi_i = [\chi_{i,1}\ \chi_{i,2}]^{\mathrm{T}} \in \Re^{2i}$ with $i \in \{x, y, z, \phi, \theta, \psi\}$ be the local state vector of ith subsystem and denoting as $u_i \in \{u_x, u_y, u_z, u_\phi, u_\theta, u_\psi\}$ its local control input. The quadrotor position and attitude dynamics, by recalling the definition of previous elements in model (9), can be rewritten in interconnected SISO state space equations as follows:

$$\begin{aligned} \dot{\chi}_{i,1} &= \chi_{i,2} \\ \dot{\chi}_{i,2} &= f_i(\chi) + g_i(\chi) u_i \\ y_i &= \chi_{i,1} \end{aligned} \tag{15}$$

where $f_i(\chi)$ and $g_i(\chi)$ are smooth functions with respect to χ which presents, respectively, the nonlinear dynamic and control functions of the ith subsystem, respectively. With

$$\begin{aligned} &f_x(\chi) = 0,\ f_y(\chi) = 0,\ f_z(\chi) = -g, \\ &f_\phi(\chi) = (I_y - I_z)/I_x \chi_{\theta,2} \chi_{\psi,2} - J_r \Omega_r / I_x \chi_{\theta,2}, \\ &f_\theta(\chi) = (I_z - I_x)/I_y \chi_{\phi,2} \chi_{\psi,2} + J_r \Omega_r / I_y \chi_{\phi,2}, \\ &f_\psi(\chi) = (I_x - I_y)/I_z \chi_{\theta,2} \chi_{\phi,2}, \\ &g_x(\chi) = 1/m,\ g_y(\chi) = 1/m,\ g_z(\chi) = c\chi_{\phi,1} c\chi_{\theta,1}/m, \\ &g_\phi(\chi) = l/I_x,\ g_\theta(\chi) = l/I_y,\ g_\psi(\chi) = 1/I_z. \end{aligned} \tag{16}$$

In order to reflect the impact of the unmodeled dynamic parts of the system and the external disturbances, considering equation model (15) with external disturbances $w_i(t)$, the above dynamic model of the quadrotor can be reformulated as follows:

$$\dot{\chi}_{i,2} = f_i(\chi) + g_i(\chi) u_i + w_i(t). \tag{17}$$

It should be mentioned that, the disturbances $w_i(t)$ are added to the model of quadrotor for considering the effects of parameters uncertainties, unmodeled dynamics and environmental flight conditions, such as aerodynamic drag force, friction and wind effects [21]. By multiplying Eq. (17) on the left by $g_i(\chi)^{-1}$, we can write each sub-model as:

$$\begin{aligned} 0 = &-g_i(\chi)^{-1} \dot{\chi}_{i,2} + g_i(\chi)^{-1} f_i(\chi) + u_i \\ &+ g_i(\chi)^{-1} w_i(t). \end{aligned} \tag{18}$$

By adding $\dot{\chi}_{i,2}$ for $i \in \{x, y, z, \phi, \theta, \psi\}$ to both sides of the equation, we can get:

$$\begin{aligned} \dot{\chi}_{i,2} = &(-g_i(\chi)^{-1} + 1)\dot{\chi}_{i,2} + g_i(\chi)^{-1} f_i(\chi) \\ &+ u_i + g_i(\chi)^{-1} w(t). \end{aligned} \tag{19}$$

If we put $\Psi_i(\chi) = (-g_i(\chi)^{-1}+1)\dot{\chi}_{i,2} + g_i(\chi)^{-1} f_i(\chi) + g_i(\chi)^{-1} w(t)$, Eq. (15) can be rewritten in the following compact form:

$$\begin{aligned} \dot{\chi}_{i,1} &= \chi_{i,2}, \\ \dot{\chi}_{i,2} &= \Psi_i(\chi) + u_i, \\ y_i &= \chi_{i,1}. \end{aligned} \tag{20}$$

Before the control design for system (15), it should be added the following assumptions.

Assumption 1 The disturbance function $w_i(t)$ is supposed unknown and bounded with slow time-varying signals. An unknown positive constant $\overline{w}_i$ exists such that $|w_i(t)| \leq \overline{w}_i$ for $i \in \{x, y, z, \phi, \theta, \psi\}$. This assumption, commonly found in many control strategies [25], is introduced to limit energetically the effect of the disturbances on the quadrotor system. In this paper, the knowledge of precise value of upper bounded disturbance is not necessary for developing our controller.

Assumption 2 The nonlinear control function $g_i(\chi) > 0$ is different from zero for the controllability purpose without changing its signal. Without losing generality, it is assumed that $g_i > 0$ for all χ. This assumption is standard for system control designing and it is made to ensure the controllability of system (15). Using Remark 1, it is easy to check that $g_i(\chi) > 0$ for all χ.

Assumption 3 The reference trajectory y_{id} for $i \in \{x, y, z, \phi, \theta, \psi\}$ and their time derivatives $\dot{y}_{id}, \ddot{y}_{id}$ are assumed to be known, smooth and bounded. As seen in [5,37], this assumption is frequently adopted to resolve the trajectory tracking problem, especially those using the backstepping method, and it is essential condition to ensure the boundedness of all closed-loop system signals.

Remark 2 Considering Assumption 3, it can guarantee the smooth variation for the nonlinear function of the dynamic position. On the other hand, the quadrotor has a symmetrical rigid body which makes the inertia factors approximately the same and the rotor inertia I_x, I_y, I_z are very small constants; hence, the variation of the nonlinear functions will be smooth for the dynamic rotation.

The position and attitude model described in (20) considers that the dynamics and external disturbances of the quadrotor are unknown which are grouped into one nonlinear function to be estimated. It is divided into six subsystems: two subsystems describe the Cartesian position dynamics, the altitude subsystem and three attitude subsystems. The unknown dynamics and external disturbance of each subsystem will be estimated using a nonlinear adaptive approximation. Based on these approximations, a nonlinear backstepping controller for trajectory tracking control problem will be designed for quadrotor system. Finally, the design parameters of the proposed controller are tuned using the cuckoo search optimization algorithm to obtain superior control performance compared to the same class of controllers.

So, our control target is to design a robust control law such that the outputs of the quadrotor system y_i track their desired smooth and bounded reference trajectories y_{id} for $i \in \{x, y, z, \phi, \theta\}$ even in the presence of unknown dynamics and external disturbances. Moreover, this control law must be able to stabilize the quadrotor subsystems until the stabilization of the overall closed-loop system and to find the most optimistic results in trajectory tracking problem. To achieve that, as shown in Fig. 2, the designed control law is applied to the quadrotor system through two cascade control loops, each with its own design objective. The first loop is related to the position control, while the second loop is devoted to the attitude stabilization. The desired trajectories for both control loops are chosen under flight objective as: The desired position trajectories (y_{xd}, y_{yd}, y_{zd}) and the desired yaw angle y_{xd} are provided by the user, whereas the desired roll and pitch trajectories $(y_{\phi d}, y_{\theta d})$ are delivered automatically from position loop by mean of Eqs. (13) and (14), as follows:

$$\begin{cases} y_{\phi d} = (u_x s y_{\psi d} - u_y c y_{\psi d})/u_z \\ y_{\theta d} = (u_x c y_{\psi d} + u_y s y_{\psi d})/u_z \end{cases}, \tag{21}$$

where u_x and u_y are generated by the proposed controller that will be developed in the next section.

Remark 3 Obviously, from Eq. (21), $y_{\phi d}$ and $y_{\theta d}$ are well defined since u_z is nonsingular, i.e., u_z is strictly positive from Eq. (3) that expresses the safely flight condition.

3 Ideal backstepping controller

The backstepping controller (BC) design methodology provides an effective tool of designing controllers for quadrotor UAV systems which has been successfully applied in several works [2,17,26]. This is due to its ability to deal with the nonlinear problems and strict mathematical proof processes. Similar to [26,37], our main purpose in this section is to develop the nonlinear BC for the closed-loop quadrotor system (20) considered that the nonlinear dynamical function $f_i(\chi)$ and the nonlinear control function $g_i(\chi)$ are known and bounded and the external disturbances $w_i(t) = 0$. The backstepping control (BC) architecture is depicted in Fig. 2.

The design of BC is described step by step with the following procedures to realize the above-mentioned objective:

Step 1. The first tracking errors are defined as follows:

$$\begin{aligned} e_{i,1} &= y_{id} - y_i \\ &= y_{id} - \chi_{i,1}, i \in \{x, y, z, \phi, \theta, \psi\}. \end{aligned} \tag{22}$$

The time derivative of (22) is given by:

$$\begin{aligned} \dot{e}_{i,1} &= \dot{y}_{id} - \dot{\chi}_{i,1} \\ &= \dot{y}_{id} - \chi_{i,2}. \end{aligned} \tag{23}$$

To ensure the stability and the convergence of the first tracking errors $e_{i,1}$, let us define the following Lyapunov function [27]:

$$V_1 = \sum_{i \in \{x,y,z,\phi,\theta,\psi\}} V_{i,1} = \frac{1}{2} \sum_{i \in \{x,y,z,\phi,\theta,\psi\}} e_{i,1}^2, \tag{24}$$

where $V_{i,1} = \frac{1}{2} e_{i,1}^2$ is a local Lyapunov function of ith subsystem. The time derivative of V_1 by substituting (22) can be found as follows:

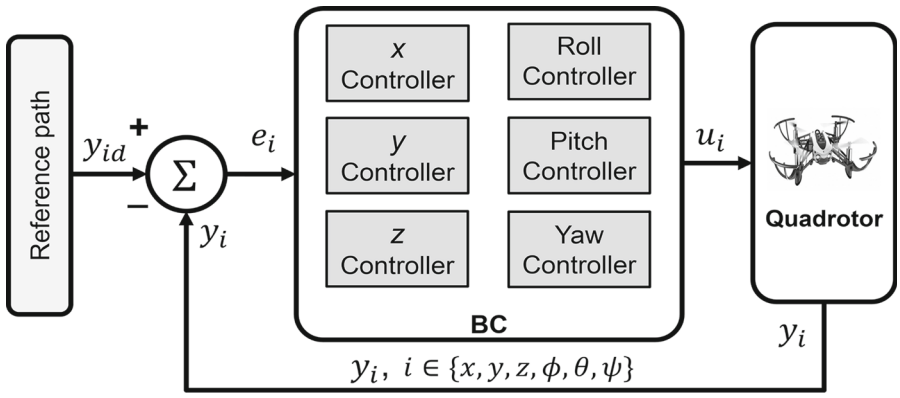

Fig. 2 Backstepping control (BC) structure

$$\dot{V}_1 = \sum_{i\in\{x,y,z,\phi,\theta,\psi\}} e_{i,1}\dot{e}_{i,1} = \sum_{i\in\{x,y,z,\phi,\theta,\psi\}} e_{i,1}(\dot{y}_{id} - \chi_{i,2}). \quad (25)$$

To satisfy the condition $\dot{V}_1$, $\chi_{i,2}$ are viewed as a virtual control inputs which can be defined as:

$$\chi_{i,2} = \dot{y}_{id} + \alpha_{i,1}e_{i,1}, \quad (26)$$

where $\alpha_{i,1}$ is a positive constant chosen by the designer. Substituting the virtual control by its desired value, (25) becomes:

$$\dot{V}_1 = -\sum_{i\in\{x,y,z,\phi,\theta,\phi\}} \alpha_{i,1}e_{i,1}^2 \leq 0. \quad (27)$$

As a result, the first error $e_{i,1}$ governed by (23) is stable and converges to zero.

Step 2. Let us define the second tracking errors:

$$e_{i,2} = \dot{\chi}_{i,1} - \chi_{i,2} = \dot{\chi}_{i,1} - \dot{y}_{id} - \alpha_{i,1}e_{i,1}. \quad (28)$$

Considering (20), the time derivative of (28) is described as follows:

$$\dot{e}_{i,2} = \ddot{\chi}_{i,1} - \ddot{y}_{id} - \alpha_{i,1}\dot{e}_{i,1} = \Psi_i(\chi) + u_i - \ddot{y}_{id} - \alpha_{i,1}\dot{e}_{i,1}. \quad (29)$$

Similar to the previous step, consider the augmented Lyapunov function for (29) given by:

$$V_2 = V_1 + \frac{1}{2}\sum_{i\in\{x,y,z,\phi,\theta,\phi\}} e_{i,2}^2 = \frac{1}{2}\sum_{i\in\{x,y,z,\phi,\theta,\phi\}} e_{i,1}^2 + e_{i,2}^2. \quad (30)$$

The time derivative of Eq. (30) with respect to time is obtained as:

$$\dot{V}_2 = \sum_{i\in\{x,y,z,\phi,\theta,\phi\}} e_{i,1}\dot{e}_{i,1} + e_{i,2}\dot{e}_{i,2} = \sum_{i\in\{x,y,z,\phi,\theta,\phi\}} e_{i,1}(\dot{y}_{id} - \dot{\chi}_{i,1}) + e_{i,2}(\ddot{\chi}_{i,1} - \dot{\chi}_{i,2}) = \sum_{i\in\{x,y,z,\phi,\theta,\phi\}} -\alpha_{i,1}e_{i,1}^2 + e_{i,2}(\Psi_i(\chi) + u_i - \ddot{y}_{id} - e_{i,1} - \alpha_{i,1}e_{i,1}). \quad (31)$$

Step 3. To ensure the stability of quadrotor system and the convergence of $e_{i,2}$ to zero, the feedback control inputs u_i are designed as follows:

$$u_i = \ddot{y}_{id} + e_{i,1} + \alpha_{i,1}\dot{e}_{i,1} - \Psi_i(\chi) - \alpha_{i,2}e_{i,2}, \quad (32)$$

where $\alpha_{i,2}$ is another designed positive constant. Using (23) and (28), one can rewrite (32) as follows:

$$u_i = \ddot{y}_{id} + (1 - \alpha_{i,1}^2)e_{i,1} + (\alpha_{i,1} + \alpha_{i,2})e_{i,2} - \Psi_i(\chi). \quad (33)$$

Substituting (32) into (31), the time derivative results in:

$$\dot{V}_2 = \sum_{i\in\{x,y,z,\phi,\theta,\psi\}} -\alpha_{i,1}e_{i,1}^2 - \alpha_{i,2}e_{i,2}^2 \leq 0. \quad (34)$$

Since $\dot{V}_2$ is semi-negative definite, the control law (33) asymptotically stabilizes system (20). As seen in (33), the designed parameters $\alpha_{i,1}$ and $\alpha_{i,2}$ define the dynamics behavior of the quadrotor tracking responses where their values are generally chosen by trial and error during the simulation tests with attention to the stability [17,20]. Moreover, the control law (33) is well defined only if the nonlinear functions $f_i(\chi)$ and $g_i(\chi)$ of quadrotor system are exactly known without subject to any parametric variations and external disturbances. However, in practice, these conditions cannot be verified and the BC has some deficiencies in realizing trajectory tracking control. For that, optimal model-free

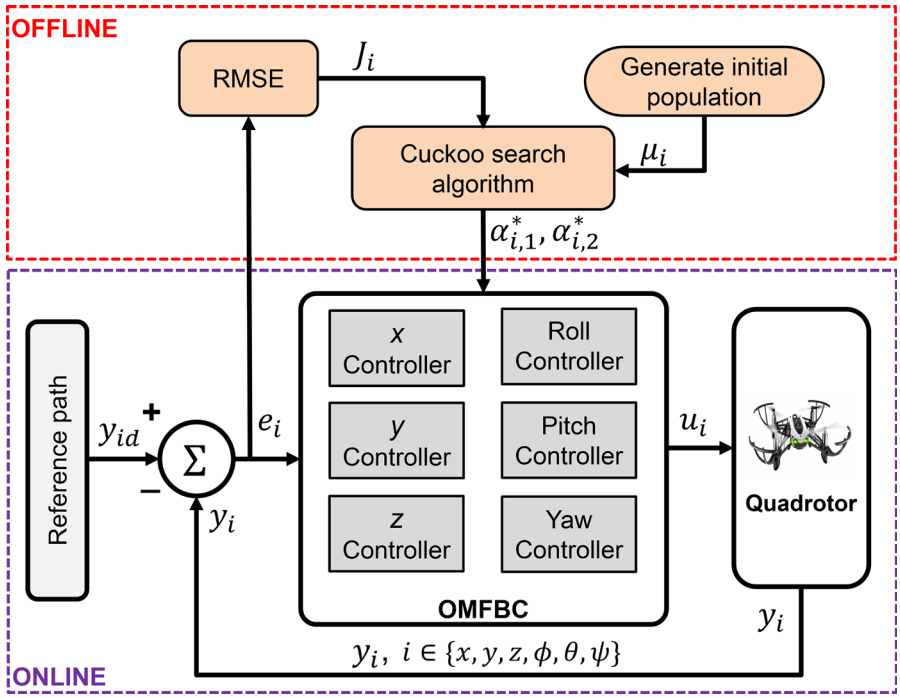

Fig. 3 Optimal model-free backstepping control (OMFBC) structure

backstepping control approaches for controlling the quadrotor are presented in the following section. The proposed control approaches consist of combining the optimized backstepping technique and adaptive nonlinear estimator to deal with unknown dynamics and external perturbations with optimized behavior.

4 Optimal model-free backstepping controller

4.1 Model-free backstepping controller

In this section, we will investigate model-free control (MFC) for quadrotor system. According to the literature [8,9], the MFC approach has several advantages which makes it favorable for many real application systems, such as the quadrotor [2,20]. The main one is that the MFC law depends only on the real-time measurement data of the controlled plant without the requirement of the precise dynamic model. However, the most of them consider that the controlled system can be represented in finite time by a very local model, in which the stability of the overall closed-loop system is not absolutely proven. Here, the main target control is to design a robust nonlinear MFBC law for each subsystem of quadrotor considering that the total dynamic functions with external disturbances are unknown, i.e., $\Psi_i(\chi)$ are unknown functions along the control path. This objective can be achieved by using the classical backstepping control law (33) combined with adaptive nonlinear estimator of $\Psi_i(\chi)$. The block diagram of the overall control system is shown in Fig. 3. Thus, the model-free counterpart of control law (33) that turns out to be that of final MFBC is defined as follows:

$$u_i = \ddot{y}_{id} + (1 - \alpha_{i,1}^2)e_{i,1} + (\alpha_{i,1} + \alpha_{i,2})e_{i,2} - \hat{\Psi}_i(\chi), \tag{35}$$

where $\hat{\Psi}_i(\chi)$ for $i \in \{x, y, z, \phi, \theta, \psi\}$ are the adaptive estimators of the total dynamic functions $\Psi_i(\chi)$.

As can be seen in (20), the unknown function estimators $\Psi_i(\chi)$ for all state variables x can be computed directly using the quadrotor velocities $x_{i,2}$ and the applied control values u_i. Different from the classic MFC theory, the estimation functions $\hat{\Psi}_i(\chi)$ in the proposed MFBC are constructed by two parts. The first part is given by the following dynamics:

$$\dot{\hat{\Psi}}_i(\chi) = \gamma_{i,1}(\chi_{i,2} - \widehat{\pi}_i), \tag{36}$$

where $\gamma_{i,1} > 0$ are the estimation parameters whose values are chosen larger than zero and $\widehat{\pi}_i$ are the adaptive factors which define the second part whose updating laws are designed as [16]:

$$\dot{\widehat{\pi}}_i = \dot{\widehat{\Psi}}_i(\chi) + u_i - \gamma_{i,2}(\widehat{\pi}_i - \chi_{i,2}), \tag{37}$$

where $\gamma_{i,2} > 0$ are other estimation parameters chosen also larger than zero.

Remark 4 The control inputs u_i designed in Eq. (35) are only related to the tracking errors $e_{i,1}$ and $e_{i,2}$ where no dynamic model information is needed. Therefore, the proposed control law is model-free without local identification, which makes it easy to be implemented in real time compared with similar works in [2,20]. Moreover, the integrating of adaptive estimators $\hat{\pi}_i$ given in (37) makes the control signal u_i to be robust against unknown dynamics and external disturbances.

Based on the above discussion, the following theorem is given to explain the MFBC performance of the overall closed-loop quadrotor system.

Theorem *Considering the control problem of quadrotor system* (20) *with satisfied assumptions* (1–3)*, the proposed model-free backstepping controller (MFBC)* (35) *consists in determining the estimators* (36) *and their adaptation laws* (37) *that ensure the stability of the overall closed-loop system and the asymptotic convergence of the tracking error toward zero, i.e.,* $\lim_{t\to+\infty} e_i(t) = 0$.

Proof To develop MFBC scheme, the proof will be introduced similarly in recursive backstepping procedure. Let us consider the following Lyapunov function candidate as:

$$V_3 = V_2 + \sum_{i\in\{x,y,z,\phi,\theta,\psi\}} \frac{1}{2\gamma_{i,2}}\tilde{\Psi}_i^2(\chi) + \frac{1}{2}\tilde{\pi}_i^2, \tag{38}$$

where $\tilde{\Psi}_i(\chi) = \Psi_i(\chi) - \hat{\Psi}_i(\chi)$ and $\tilde{\pi}_i = \chi_{i,2} - \hat{\pi}_i$ represents the estimation errors of the unknown functions and the adaptive factors, respectively.

The chosen Lyapunov candidate function is composed of three terms. The first term is chosen to guarantee that the all quadrotor outputs will asymptotically track the desired trajectories. Moreover, it ensures asymptotic stability of the overall closed-loop system according to the proposed control method. The second term is added to establish the adaptive law for online tuning of the estimators that approximate the unknown nonlinear functions. Finally, the update law for the adaptive factors of the estimators is derived from the last term. The time derivative of V_3 along the solution of (29) is:

$$\begin{aligned}\dot{V}_3 &= \dot{V}_2 + \sum_{i\in\{x,y,z,\phi,\theta,\psi\}} \frac{1}{\gamma_{i,1}}\tilde{\Psi}_i(\chi)\dot{\tilde{\Psi}}_i(\chi) + \tilde{\pi}_i\dot{\tilde{\pi}}_i \\ &= \sum_{i\in\{x,y,z,\phi,\theta,\psi\}} e_{i,1}\dot{e}_{i,1} + e_{i,2}\dot{e}_{i,2} \\ &\quad + \sum_{i\in\{x,y,z,\phi,\theta,\psi\}} \frac{1}{\gamma_{i,1}}\tilde{\Psi}_i(\chi)\left(\dot{\Psi}_i(\chi) - \dot{\hat{\Psi}}_i(\chi)\right) \\ &\quad + \tilde{\pi}_i\left(\dot{\chi}_{i,2} - \dot{\hat{\pi}}_i\right). \end{aligned} \tag{39}$$

Considering Remark 2, the unknown function of each subsystem has a smooth variation, which leads to neglecting its derivative, i.e., $\dot{\Psi} \approx 0$. Using (31), one has:

$$\begin{aligned}\dot{V}_3 &= \sum_{i\in\{x,y,z,\phi,\theta,\psi\}} -\alpha_{i,1}e_{i,1}^2 + e_{i,2}(\Psi_i(\chi) \\ &\quad + u_i - \ddot{y}_{id} - e_{i,1} - \alpha_{i,1}\dot{e}_{i,1}) \\ &\quad + \sum_{i\in\{x,y,z,\phi,\theta,\psi\}} -\frac{1}{\gamma_{i,1}}\tilde{\Psi}_i(\chi)\dot{\hat{\Psi}}_i(\chi) \\ &\quad + \tilde{\pi}_i(\dot{\chi}_{i,2} - \dot{\hat{\pi}}_1). \end{aligned} \tag{40}$$

Considering (23) and (28), (40) becomes

$$\begin{aligned}\dot{V}_3 &= \sum_{i\in\{x,y,z,\phi,\theta,\psi\}} -\alpha_{i,1}e_{i,1}^2 \\ &\quad + \sum_{i\in\{x,y,z,\phi,\theta,\psi\}} e_{i,2}(\Psi_i(\chi) + u_i - \ddot{y}_{id} \\ &\quad - (\alpha_{i,1} + \alpha_{i,2})e_{i,2} + (\alpha_{i,1}^2 - 1)e_{i,1}) \\ &\quad + \sum_{i\in\{x,y,z,\phi,\theta,\psi\}} -\frac{1}{\gamma_{i,1}}\tilde{\Psi}_i(\chi)\dot{\hat{\Psi}}_i(\chi) \\ &\quad + \tilde{\pi}_i(\dot{\chi}_{i,2} - \dot{\hat{\pi}}_1). \end{aligned} \tag{41}$$

Substituting (35) in (41) yields:

$$\begin{aligned}\dot{V}_3 &= \sum_{i\in\{x,y,z,\phi,\theta,\psi\}} -\alpha_{i,1}{e_{i,1}}^2 - \alpha_{i,2}{e_{i,2}}^2 \\ &\quad + \sum_{i\in\{x,y,z,\phi,\theta,\psi\}} -\frac{1}{\gamma_{i,1}}\tilde{\Psi}_i(\chi)\dot{\hat{\Psi}}_i(\chi) \\ &\quad + \tilde{\pi}_i(\dot{\chi}_{i,2} - \dot{\hat{\pi}}_1). \end{aligned} \tag{42}$$

Invoking (36) and (37), the time derivative of V_3 becomes:

$$\begin{aligned}\dot{V}_3 &= \sum_{i\in\{x,y,z,\phi,\theta,\psi\}} -\alpha_{i,1}{e_{i,1}}^2 - \alpha_{i,2}{e_{i,2}}^2 \\ &\quad - \frac{1}{\gamma_{i,1}}\gamma_{i,1}\tilde{\Psi}_i(\chi)(\chi_{i,2} - \hat{\pi}_i) \\ &\quad + \tilde{\pi}_i(\dot{\chi}_{i,2} - (\dot{\hat{\Psi}}_i(\chi) + u_i - \gamma_{i,2}(\hat{\pi}_i - \chi_{i,2}))) \end{aligned}$$

$$= \sum_{i\in\{x,y,z,\phi,\theta,\psi\}} -\alpha_{i,1}{e_{i,1}}^2 - \alpha_{i,2}{e_{i,2}}^2 - \tilde{\Psi}_i(\chi)\tilde{\pi}_i + \tilde{\pi}_i(\dot{\chi}_{i,2} - (\widehat{\Psi}_i(\chi) + u_i - \gamma_{i,2}(\widehat{\pi}_i - \chi_{i,2}))). \tag{43}$$

Substituting (20) into (43) gives:

$$\dot{V}_3 = \sum_{i\in\{x,y,z,\phi,\theta,\psi\}} -\alpha_{i,1}{e_{i,1}}^2 - \alpha_{i,2}{e_{i,2}}^2 - \tilde{\Psi}_i(\chi)\tilde{\pi}_i + \sum_{i\in\{x,y,z,\phi,\theta,\psi\}} \tilde{\pi}_i(\Psi_i(\chi) + u_i - (\hat{\Psi}_i(\chi) + u_i - \gamma_{i,2}(\widehat{\pi}_i - \chi_{i,2}))). \tag{44}$$

After some mathematical simplifications, $\dot{V}_3$ can be rewritten as:

$$\dot{V}_3 = \sum_{i\in\{x,y,z,\phi,\theta,\psi\}} -\alpha_{i,1}e_{i,1}^2 - \alpha_{i,2}e_{i,2}^2 - \tilde{\Psi}_i(\chi)\tilde{\pi}_i + \tilde{\pi}_i(\tilde{\Psi}_i(\chi) - \gamma_{i,2}\tilde{\pi}_i) \tag{45}$$

$$\dot{V}_3 = \sum_{i\in\{x,y,z,\phi,\theta,\psi\}} -\alpha_{i,1}e_{i,1}^2 - \alpha_{i,2}e_{i,2}^2 - \gamma_{i,2}\tilde{\pi}_i^2 \leq 0. \tag{46}$$

Since $\alpha_{i,1}$, $\alpha_{i,2}$ and $\gamma_{i,2}$ are positive constants, it could get $\dot{V}_3$ is a semi-negative definite function and $V_3 \in L_\infty$. This implies that the stability of the MFBC closed-loop system of quadrotor can be guaranteed and the signals $e_{i,1}$, $e_{i,2}$, $\tilde{\Psi}_i$ and $\tilde{\pi}_i$ are bounded. Moreover, by using Barbalat's lemma [38], one can conclude that the values of the tracking errors $e_{i,1}$ and $e_{i,2}$ converge asymptotically to zero. Thus, the theorem is proved. □

Remark 5 The overall quadrotor seen as a large-scale system represented by (15) is stabilized by selecting virtual control inputs as (26) and the MFC law as (35). The asymptotic convergence of the outputs y_i, position and attitude, to the desired trajectories y_{id} is achieved by using the multiple Lyapunov functions as (30) and (38), i.e., $V = \sum V_i$ for $i \in \{x, y, z, \phi, \theta, \psi\}$. As a result, the stability of the entire system can be ensured. This idea provides a new solution to construct the candidate Lyapunov function for control problem of the quadrotor and similar application systems. Moreover, the problem of explosion and complexity in backstepping control technique is avoided since it is applied to the lower-dimensional subsystems. Indeed, the model-free backstepping designed controller has more advantages such as more degrees of freedom in the control parameters, simpler updating laws and being expected to achieve better control performance.

4.1.1 Attitude control

The quadrotor has three rotational motions that allow to transit from normal mode to inverted mode or vice versa according to the ith subsystem for each angle. The roll subsystem is:

$$\begin{aligned} \dot{\chi}_{\phi,1} &= \chi_{\phi,2} \\ \dot{\chi}_{\phi,2} &= \Psi_\phi(\chi) + u_\phi \\ y_\phi &= \chi_{\phi,1}, \end{aligned} \tag{47}$$

where u_ϕ is the control input signal of the roll subsystem defined as:

$$\begin{cases} u_\phi = \ddot{y}_{\phi\,d} + (1-\alpha_{\phi,1}^2)e_{\phi,1} + (\alpha_{\phi,1}+\alpha_{\phi,2})e_{\phi,2} - \hat{\Psi}_\phi(\chi) \\ \dot{\hat{\Psi}}_\phi(\chi) = \gamma_{\phi,1}(\chi_{\phi,2} - \widehat{\pi}_\phi) \\ \dot{\widehat{\pi}}_\phi = \widehat{\Psi}_\phi(\chi) + u_\phi - \gamma_{\phi,1}(\widehat{\pi}_\phi - \chi_{\phi,2}) \end{cases}. \tag{48}$$

The pitch subsystem is:

$$\begin{aligned} \dot{\chi}_{\theta,1} &= \chi_{\theta,2}, \\ \dot{\chi}_{\theta,2} &= \Psi_\theta(\chi) + u_\theta, \\ y_\theta &= \chi_{\theta,1}, \end{aligned} \tag{49}$$

where u_θ is the control input signal of the pitch subsystem defined as:

$$\begin{cases} u_\theta = \ddot{y}_{\theta\,d} + (1-\alpha_{\theta,1}^2)e_{\theta,1} + (\alpha_{\theta,1}+\alpha_{\theta,2})e_{\theta,2} - \hat{\Psi}_\theta(\chi) \\ \dot{\hat{\Psi}}_\theta(\chi) = \gamma_{\theta,1}(\chi_{\theta,2} - \widehat{\pi}_\theta) \\ \dot{\widehat{\pi}}_\theta = \widehat{\Psi}_\theta(\chi) + u_\theta - \gamma_{\theta,1}(\widehat{\pi}_\theta - \chi_{\theta,2}) \end{cases}. \tag{50}$$

The yaw subsystem is:

$$\begin{aligned} \dot{\chi}_{\psi,1} &= \chi_{\psi,2}, \\ \dot{\chi}_{\psi,2} &= \Psi_\theta(\chi) + u_\psi, \\ y_\psi &= \chi_{\psi,1}, \end{aligned} \tag{51}$$

where u_θ is the control input signal of the pitch subsystem defined as:

$$\begin{cases} u_\theta = \ddot{y}_{\theta\,d} + (1-\alpha_{\theta,1}^2)e_{\theta,1} + (\alpha_{\theta,1}+\alpha_{\theta,2})e_{\theta,2} - \hat{\Psi}_\theta(\chi) \\ \dot{\hat{\Psi}}_\theta(\chi) = \gamma_{\theta,1}(\chi_{\theta,2} - \widehat{\pi}_\theta) \\ \dot{\widehat{\pi}}_\theta = \widehat{\Psi}_\theta(\chi) + u_\theta - \gamma_{\theta,1}(\widehat{\pi}_\theta - \chi_{\theta,2}) \end{cases}. \tag{52}$$

4.1.2 Position control

The quadrotor helicopter can be hovering at a certain altitude z, where the dynamic model of the altitude subsystem can be defined as:

$$\dot{\chi}_{z,1} = \chi_{z,2},$$

$$\begin{aligned}\dot{\chi}_{z,2} &= \Psi_z(\chi) + u_z,\\ y_z &= \chi_{z,1},\end{aligned} \tag{53}$$

where u_z is the control input signal of the altitude subsystem defined as:

$$\begin{cases} u_z = \ddot{y}_{zd} + (1-\alpha_{z,1}^2)e_{z,1} + (\alpha_{z,1}+\alpha_{z,2})e_{z,2} - \hat{\Psi}_z(\chi) \\ \dot{\hat{\Psi}}_z(\chi) = \gamma_{z,1}(\chi_{z,2} - \hat{\pi}_z) \\ \dot{\hat{\pi}}_z = \dot{\hat{\Psi}}_z(\chi) + u_z - \gamma_{z,1}(\hat{\pi}_z - \chi_{z,2}) \end{cases} \tag{54}$$

In order that the quadrotor tracks its desired path in x and y plan, virtual control inputs u_x and u_y of Cartesien position subsystems are designed as:

$$\begin{cases} u_x = \ddot{y}_{xd} + (1-\alpha_{x,1}^2)e_{x,1} + (\alpha_{x,1}+\alpha_{x,2})e_{x,2} - \hat{\Psi}_x(\chi) \\ u_y = \ddot{y}_{yd} + (1-\alpha_{y,1}^2)e_{y,1} + (\alpha_{y,1}+\alpha_{y,2})e_{y,2} - \hat{\Psi}_y(\chi) \end{cases} \tag{55}$$

with:

$$\begin{cases} \dot{\hat{\Psi}}_x(\chi) = \gamma_{x,1}(\chi_{x,2} - \hat{\pi}_x) \\ \dot{\hat{\pi}}_x = \dot{\hat{\Psi}}_x(\chi) + u_x - \gamma_{x,1}(\hat{\pi}_x - \chi_{x,2}) \\ \dot{\hat{\Psi}}_y(\chi) = \gamma_{y,1}(\chi_{y,2} - \hat{\pi}_y) \\ \dot{\hat{\pi}}_y = \dot{\hat{\Psi}}_y(\chi) + u_y - \gamma_{y,1}(\hat{\pi}_i - \chi_{y,2}) \end{cases}. \tag{56}$$

4.2 CSA-model-free backstepping controller

In this part, we propose to use the metaheuristic cuckoo search algorithm (CSA) to compute the optimal parameters of the proposed control law. The CSA is a computational algorithm which optimizes many specific problems by iteratively trying to enhance a candidate solution against a given cost function. The aim for using cuckoo search algorithm is to determine the optimal proposed control law by selecting the optimal values $\alpha_{i,1}^*$ and $\alpha_{i,2}^*$ for $i \in \{x, y, z, \phi, \theta, \psi\}$ of the backstepping control law in Eq. (33), and it needs to be positive to satisfy stability criteria.

Algorithm 1 Pseudo-code of the cuckoo search algorithm

```
Cost function Min J_i for i ∈ {x, y, z, φ, θ, ψ}
Initialize n population of host nests μ_{i-1} ∈ {α_{i,1}, α_{i,2}}
while t < Max Generation do
  Evaluate the local random search μ_i by Lévly flights.
  Generate new solution using the global search. Equation (58)

  A fraction of worse nests are abandoned via probability factor p_a to build new ones q_j. Equation (59)
  Evaluate the cost function J(q_j)
  if J(q_j) < J(μ_{j-1}) then
    Replace by the new solution q_j. Equation (60)
  end if
  Keep the best solutions (or nests with quality solutions).
end while
Rank the solutions and find the current best.
```

The cuckoo search algorithm steps are summarized in Algorithm 1, and the flowchart of CSA is depicted in Fig. 4. The proposed algorithm searches for the best solution used local μ_j and global v_j random search nests which contain random values of the parameters required to be optimized and controlled by the probability parameter p_a at each generation j. The CSA parameters are summarized in Table 1.

$$\mu_j = \mu_{j-1} + \delta s \otimes H(p_a - \varepsilon) \otimes (\mu_{j-1}^p - \mu_{j-1}^r) \tag{57}$$

$$v_i = \mu_i + \delta L(s, \lambda), \tag{58}$$

where $\otimes$ denotes entry-wise product of two vectors, δ is positive step size scaling factor, s is the step size, H is a Heavy-side function [24], $\varepsilon \in [0, 1]$ is a random number, μ_j^p and μ_j^r two different solutions are selected randomly, and $L(s, \lambda)$ represents lévely flights distribution used to define the step size of random walk. The local and global random walk is controlled by probability factor as:

$$q_j = \begin{cases} \mu_j & \text{if rand}(0, 1) > p_a \\ v_j & \text{otherwise} \end{cases}. \tag{59}$$

The best solution will be selected using a cost function condition:

$$\mu_j^{\text{best}} = \begin{cases} q_j & \text{if } \mathrm{J}(q_j) < \mathrm{J}(\mu_{j-1}) \\ \mu_j & \text{otherwise} \end{cases}. \tag{60}$$

In the present study, the cost function J_i of the optimization algorithm should be minimized through the optimization problem, which includes different performance criteria. For this need, several objective function forms are used in the literature such as the mean squared error (MSE) [22,39], the integral time absolute error (ITAE) [49], the individual absolute error (IAE) [35] and the integral square error (ISE) [43]. On the other hand, the root-mean-square error (RMSE) is the most commonly used cost function to assess individuals [3,11,34]. In this work, the RMSE between the desired and the actual outputs is used to evaluate the performance of the controller (Algorithm 1). The RMSE criterion can be defined mathematically as:

$$J_i = \sqrt{\frac{\sum_{j=1}^{N} (y_{id} - \chi_{i,1})^2}{N}} \tag{61}$$

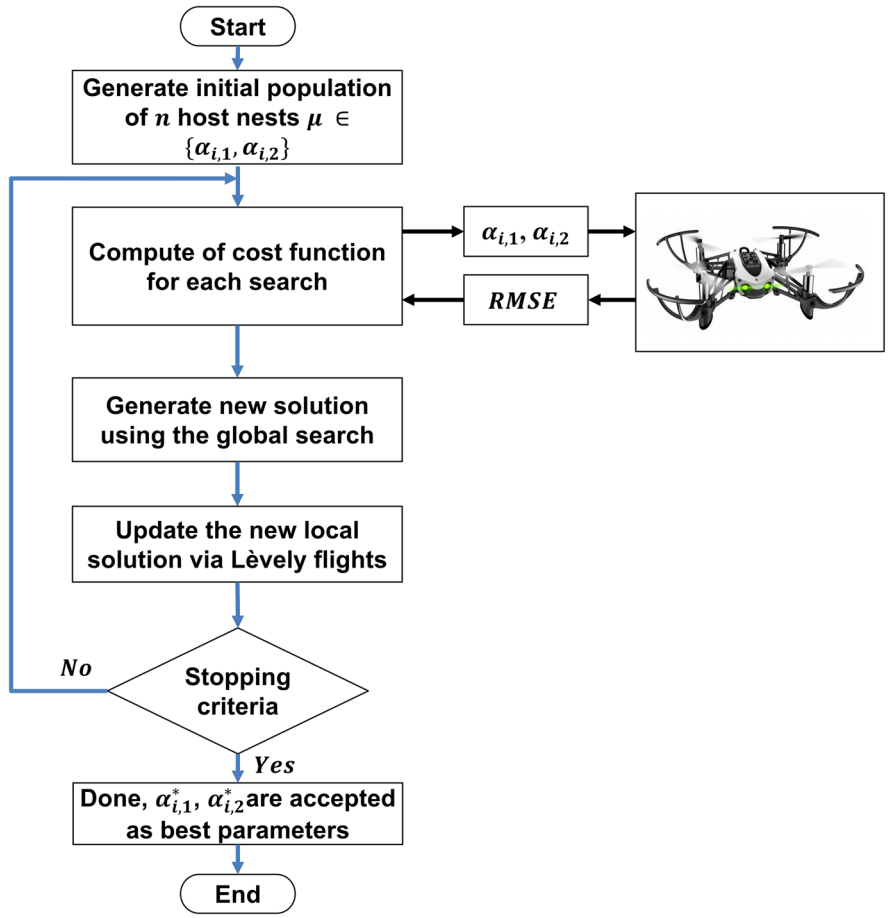

Fig. 4 Flowchart of cuckoo search process

with N is the sampling time size and $i \in \{x, y, z, \phi, \theta, \psi\}$.

Since the subsystems χ_x and χ_y have the same mathematical structure, the RMSE is taken as $J_{x,y} = \frac{J_x + J_y}{2}$. Meanwhile, the RMSE for the rotation subsystems χ_ϕ and χ_θ is taken as $J_{\phi,\theta} = \frac{J_\phi + J_\theta}{2}$, where the subscripts are denoted for roll and pitch.

The quadrotor system model is carried out for the simulation phase to calculate of the cost function J_i. The main objective is to minimize these cost function values in order to improve the system response to steady-state errors.

Remark 6 The CSA is applied to a MFBC to achieve a better performance for quadrotor UAV according to some predefined objectives like minimizing the RMSE objective function. It has been proved to be effective and more advantageous in comparison with other metaheuristic optimization algorithms, such as GA [13] and PSO algorithm [7,27]. The CSA is characterized by its simplicity, high convergence speed and its tuning procedure of the controller design parameters which allows not only to eliminate the requirement of expertise needed for setting these parameters but also to obtain a robust and accurate MFBC [18,45]. The performance and the precision of the CSA are not influenced by its parameters (n, P_a, δ, s) given in Table 1; however, it is necessary to make a judicious choice of the search space $\alpha_{i,1}, \alpha_{i,2} \in [\mu_i^{\min}, \mu_i^{\max}]$. The limits $\mu_i^{\min}$ and $\mu_i^{\max}$ are selected generally by the user during simulation tests, and their values should satisfy the

Table 1 CSA parameters

Parameters	Symbol	Value
Number of nests	n	25
Fraction of nests	P_a	0.25
Step size scaling factor	δ	1.5
Step size	s	0.01

Table 2 Parameters of the quadrotor

Parameters	Value
I_x	7.5×10^{-3} kg m^2
I_y	7.5×10^{-3} kg m^2
I_z	1.3×10^{-2} kg m^2
J_r	6×10^{-5} kg m^2
g	9.81 m/s^2
l	0.23 m
m	0.65 kg
k_b	3.1×10^{-5} N s^2
k_d	7.5×10^{-7} N m s^2

Table 3 Control gains

Controllers	x, y	z	ϕ	ψ
BC	$\alpha_1 = 5.5$	$\alpha_1 = 5.5$	$\alpha_1 = 4$	$\alpha_1 = 3.75$
	$\alpha_2 = 2.75$	$\alpha_2 = 2.75$	$\alpha_2 = 2.25$	$\alpha_2 = 1.5$
OMFBC	$\alpha_1^* = 3.9551$	$\alpha_1^* = 3.9551$	$\alpha_1^* = 6.0706$	$\alpha_1^* = 6.0706$
	$\alpha_2^* = 5.9116$	$\alpha_2^* = 5.91165$	$\alpha_2^* = 6.9681$	$\alpha_2^* = 6.9681$
	$\gamma_1 = 900$	$\gamma_1 = 500$	$\gamma_1 = 300$	$\gamma_1 = 300$
	$\gamma_2 = 100$	$\gamma_2 = 100$	$\gamma_2 = 90$	$\gamma_2 = 90$

stability condition. The RMSE criteria (61) between the desired and the actual quadrotor position and attitude outputs are used to evaluate the performance of the proposed controller. This is achieved through the search of optimal values of $\alpha_{i,1}^*$ and $\alpha_{i,2}^*$ according to steps of the flowchart 4.

Apparently, the proposed method can also be extensively applied in numerous fields' areas such as electrical engineering, electronics engineering and mechanical engineering, in which the application system must be represented as the form (15). Besides, under some assumptions, the proposed method can also be extended to the case of systems with the unknown dynamics and subject to actuator and/or sensor faults [5]. In this case, a model-free fault-tolerant control can be studied with some restrictions related to the kind of actuator and/or sensor faults. So, the similar result can be obtained with a minor change of the estimator functions $\Psi_i(\chi)$ and their updating laws. Otherwise, it has been shown in the literature [10,37] that using neural networks and/or fuzzy systems as universal approximators in control of MIMO nonlinear systems gives interesting results.

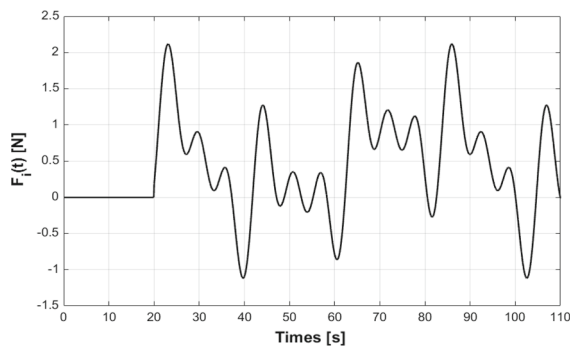

Fig. 5 External force function

So, they can be employed in new control schemes to improve the quadrotor performances.

5 Numerical results

To show the performance of the proposed control scheme, MATLAB software and the Simulink environment have been used to implement the corresponding control algorithm. The proposed controller (OMFBC) is compared with the classical BC. The parameters of

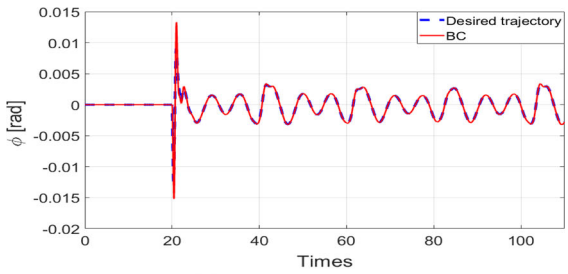

(a) Roll subsystem response.

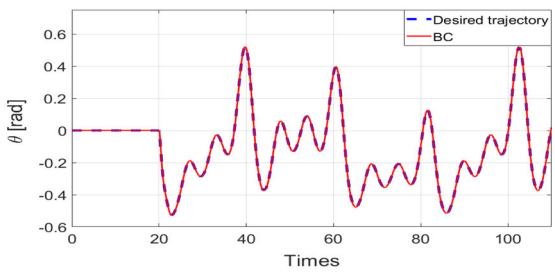

(b) Pitch subsystem response.

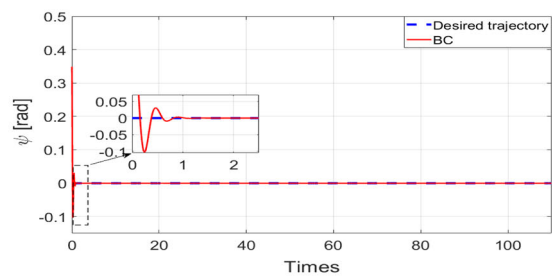

(c) Yaw subsystem response.

Fig. 6 Attitude response of the quadrotor controlled with BC (Case 1)

the quadrotor used in the following simulations are shown in Table 2 which are chosen from the tests in [20]. The disturbances have been considered in all of these simulations to test the robustness of the proposed algorithm. Firstly, the parameters of the proposed controller have been optimized against the cost function J_i for $i \in \{x, y, z, \phi, \theta, \psi\}$ in bounded search space $\mu_i \in [\mu_i^{\min}, \mu_i^{\max}] = [1, 10]$ by satisfying the stability condition. Using Remark 2, the same control parameters obtained from the CSA can be used for the position subsystems (i.e., x, y and z), where RMSE for the position subsystems is chosen as RMSE-P $= \sum_{i\in\{x,y,z\}} J_i$, and the same control parameters obtained from the CSA for the rotation subsystem (i.e., ϕ, θ and ψ) where the RMSE for the rotation subsystems is chosen as RMSE-R $= \sum_{i\in\{\phi,\theta,\phi\}} J_i$.

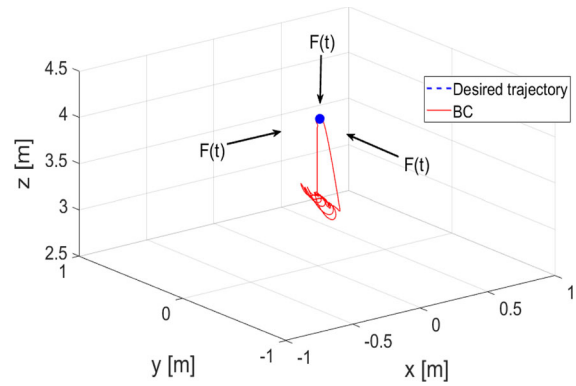

Fig. 7 3D space for the quadrotor with BC under external forces (Case 1)

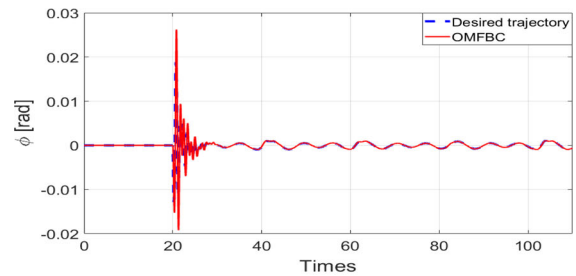

(a) Roll subsystem response.

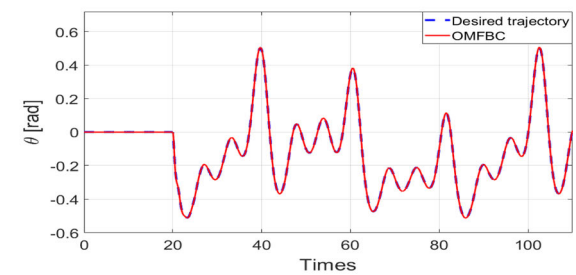

(b) Pitch subsystem response.

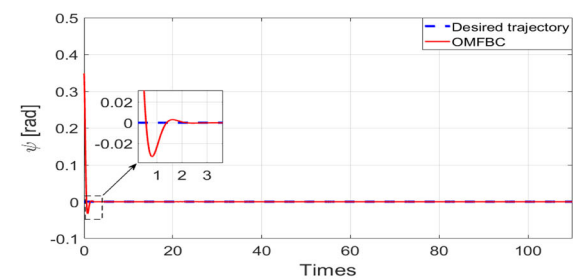

(c) Yaw subsystem response.

Fig. 8 Attitude response of the quadrotor controlled with OMFBC (Case 1)

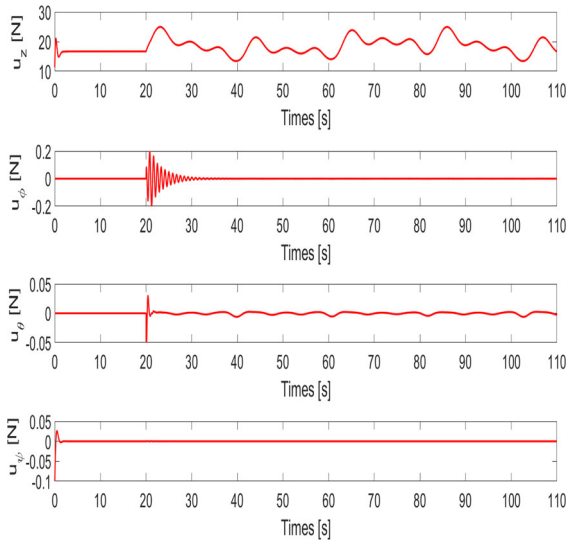

Fig. 9 Control inputs of OMFBC (Case 1)

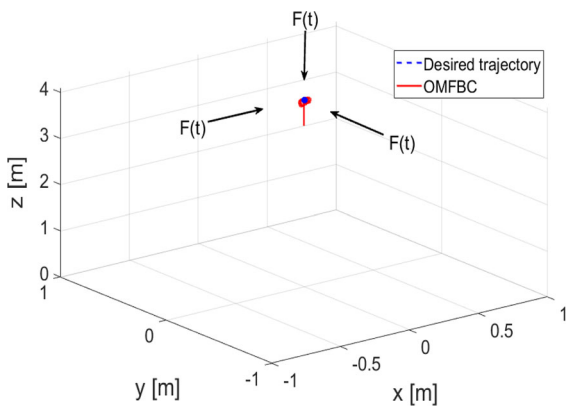

Fig. 10 3D space for the quadrotor with OMFBC under external forces (Case 1)

The controller parameters of the proposed OMFBC and BC are listed in Table 3. The simulation results were obtained for two different cases. The force disturbances $F(t)$ among the linear position are shown in Fig. 5 which are imposed on the quadrotor for $t > 20$ s in both cases.

Case 1: Stability performances under external forces

In this simulation test, the results of the proposed controller in stabilizing case are obtained for stable hovering state. The desired trajectory is defined as: $y_{xd} = 0$ m, $y_{yd} = 0$ m, $y_{zd} = 4$ m, $y_{\psi d} = 0$ rad. The initial

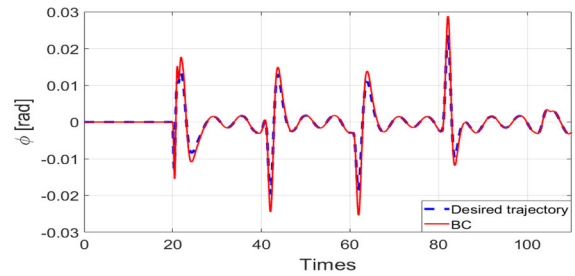

(a) Roll subsystem response.

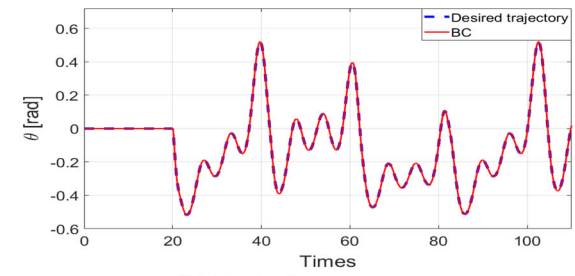

(b) Pitch subsystem response.

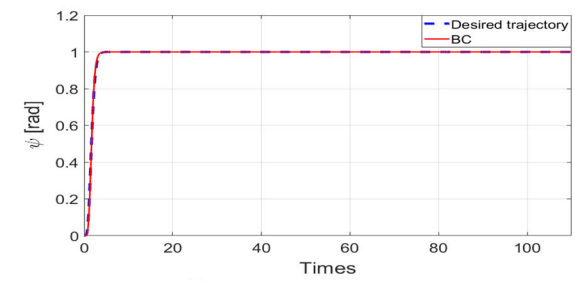

(c) Yaw subsystem response.

Fig. 11 Attitude response of the quadrotor controlled with BC (Case 2)

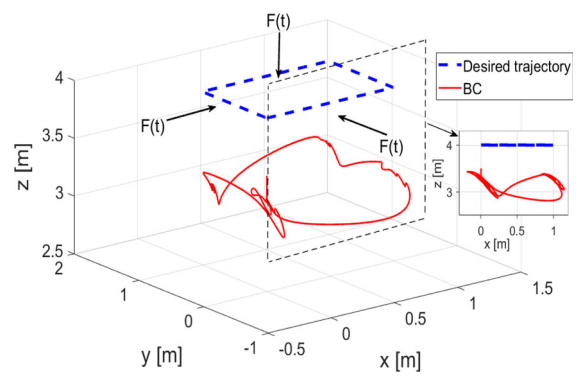

Fig. 12 3D space for the quadrotor with BC under external forces (Case 2)

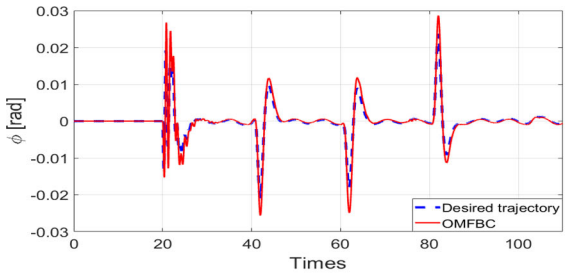

(a) Roll subsystem response.

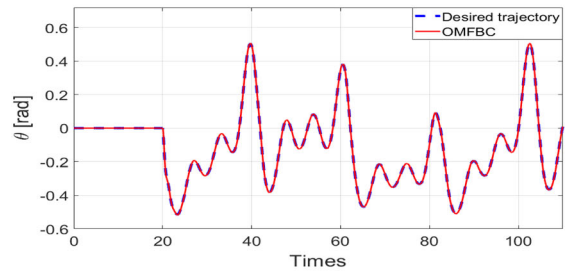

(b) Pitch subsystem response.

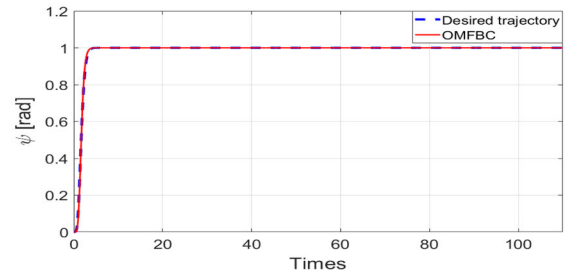

(c) Yaw subsystem response.

Fig. 13 Attitude response of the quadrotor controlled with OMFBC (Case 2)

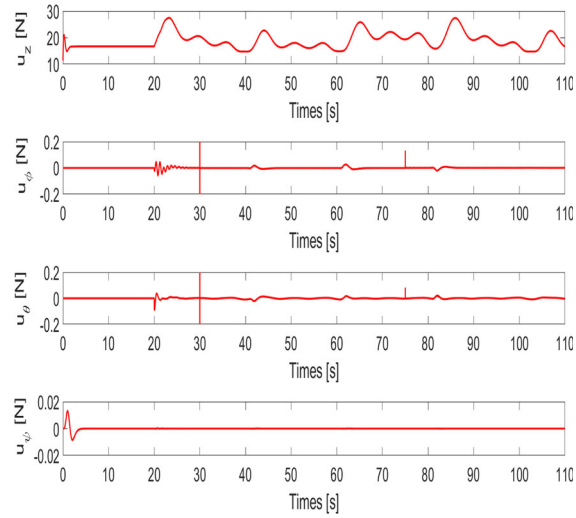

Fig. 14 Control inputs of OMFBC (Case 2)

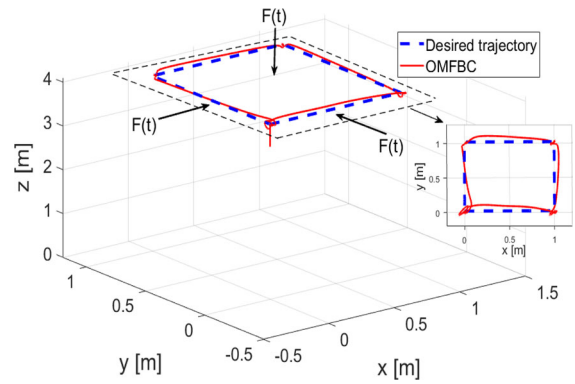

Fig. 15 3D space for the quadrotor with OMFBC under external forces (Case 2)

position of the quadrotor was: $\wp_0 = [0, 0, 3.5]^{\mathrm{T}}$ m with respect to initially hovering certain altitude without moving, the initial rotation was $\Phi_0 = [0, 0, 0.34]^{\mathrm{T}}$ rad, the initial position velocity was $\xi_0 = [0, 0, 0]^{\mathrm{T}}$ m/s, and the initial rotation velocity was $\omega_0 = [0, 0, 0]^{\mathrm{T}}$ rad/s.

The response of the angles attitude for stabilizing scenario controlled with BC is depicted in Fig. 6. The numerical results for stabilizing a quadrotor are depicted in 3D plot as shown in Fig. 7, where it can be seen that the BC has less effectiveness for stabilizing the quadrotor under external forces; so, the null tracking error cannot be reached with backstepping controller.

Figures 8 and 9 show the attitude tracking results and the input signals, respectively, using the proposed OMFBC when hovering over a fixed point under external forces introduced at $t = 20$ s. It can be seen that the inputs signal has a smooth variation. The 3D plot of the simulation results for the quadrotor stabilization under external forces using OMFBC is depicted in Fig. 10. It shows that the quadrotor can hover stably neglecting tracking errors. This illustrates that the proposed controller (OMFBC) is successfully handling the effect of external disturbances keeping the hovering capability.

Case 2: Trajectory tracking performances under external forces

In this case, the quadrotor is assumed in hovering state and tracking for the designed trajectory under external

forces $F(t)$. The desired trajectory is made up of a set of line stretches (Square trajectory) with altitude $y_{zd} = 4\,\text{m}$ and $y_{\psi d} = 1\,\text{rad}$ as:

$$y_{xd} = \begin{cases} 0\,\text{m}, & t < 20\,\text{s} \\ 1\,\text{m}, & 20\,\text{s} \le t < 40\,\text{s} \\ 1\,\text{m}, & 40\,\text{s} \le t < 60\,\text{s} \\ 0\,\text{m}, & 60\,\text{s} \le t < 80\,\text{s} \\ 0\,\text{m}, & 80\,\text{s} \le t \end{cases},$$

$$y_{yd} = \begin{cases} 0\,\text{m}, & t < 20\,\text{s} \\ 0\,\text{m}, & 20\,\text{s} \le t < 40\,\text{s} \\ 1\,\text{m}, & 40\,\text{s} \le t < 60\,\text{s} \\ 1\,\text{m}, & 60\,\text{s} \le t < 80\,\text{s} \\ 0\,\text{m}, & 80\,\text{s} \le t \end{cases}.$$

The initial position of the quadrotor was: $\wp_0 = [0, 0, 3.5]^{\text{T}}\,\text{m}$, the initial rotation was $\Phi_0 = [0, 0, 0]^{\text{T}}\,\text{rad}$, the initial position velocity was $\xi_0 = [0, 0, 0]^{\text{T}}\,\text{m/s}$, and the initial rotation velocity was $\omega_0 = [0, 0, 0]^{\text{T}}\,\text{rad/s}$.

The disturbances and controller parameters used in this case are the same as those in Case 1. The attitude angles response is shown in Fig. 11. The trajectory tracking results are depicted as 3D space in Fig. 12. It illustrates that the ideal backstepping control strategy failed for tracking the desired path.

For testing the performance of the proposed OMFBC, the same simulation was applied on the quadrotor with the same condition. Figures 13 and 14 show the tracking attitude angles and the control signal, respectively. It can be seen that the actual angles track the desired angles trajectory, regardless of the disturbances and the initial attitude errors. The simulation results of the position tracking for OMFBC approach under the occurrence of external disturbances are shown in Fig. 15. As it can be seen, the quadrotor is still able to track the desired path.

The above simulation results demonstrate that the proposed optimal model-free backstepping controller (OMFBC) has better tracking performance than ideal backstepping controller (BC). Due to the proposed observer and the optimization strategy (CSA) to identify the optimal parameters, the external disturbances such as external forces are well compensated. To investigate the performance of the designed controllers more quantitatively, the RMSE and the maximum absolute values of the tracking errors (MaxAE) for both cases were also calculated and are summarized in Table 4. Thus, these tests demonstrate clearly the good performance and robustness properties of the proposed OMFBC with respect to the BC. Note that the maximum absolute tracking error for the desired rotation angles is similar for both BC and OMFBC controllers since the disturbances are applied only on the position subsystems.

6 Conclusion

In this investigation, an optimal model-free backstepping controller (OMFBC) has been developed to be applied to the quadrotor system, whose dynamics look like a helicopter. The extracted model of quadrotor has been decoupled into six multi-input–multi-output (MIMO) subsystems where the proposed OMFBC is applied for each of them. Model-free backstepping approach and cuckoo search algorithm are used to develop an optimal control law to deal with unknown system dynamics and external disturbances according to the Lyapunov stability analysis. This approach which may be applied on limited knowledge model is simple to implement. The results obtained by applying the proposed controller in simulation environment demonstrate clearly the good performance and robustness property of the proposed OMFBC with respect to the BC, from which we can conclude the effectiveness of such controller. Our future research topics will focus on the current works such as piecewise affine (PWA)

Table 4 Values of the mean square error criteria (RMSE) and the maximum absolute error (MaxAE) of the proposed OMFBC and BC

Controller	Subsystem	RMSE		MaxAE	
		Case 1	Case 2	Case 1	Case 2
BC	Rotation (rad)	9.1×10^{-3}	1.5×10^{-2}	0.349	0.349
	Position (m)	7.584×10^{-1}	1.027	0.59	0.592
OMFBC	Rotation (rad)	3.8×10^{-3}	4×10^{-3}	0.35	0.341
	Position (m)	6.4×10^{-2}	6.38×10^{-2}	0.45	0.46

and adaptive controllers [50,51] for the quadrotor and give a comparison to the nonlinear control laws including different optimization algorithms.

Acknowledgements The authors acknowledge the support of the University of Biskra. This work was supported also by the Algerian Ministry of Higher Education and Scientific Research.

Compliance with ethical standards

Conflict of interest The authors declare that they have no conflict of interest.

References

1. Aboudonia, A., El-Badawy, A., Rashad, R.: Disturbance observer-based feedback linearization control of an unmanned quadrotor helicopter. Proc. Inst. Mech. Eng. Part I: J. Syst. Control Eng. **230**(9), 877–891 (2016)
2. Al Younes, Y., Drak, A., Noura, H., Rabhi, A., El Hajjaji, A.: Robust model-free control applied to a quadrotor uav. J. Intell. Robot. Syst. **84**(1–4), 37–52 (2016)
3. Alrashidi, M., Rahman, S., Pipattanasomporn, M.: Metaheuristic optimization algorithms to estimate statistical distribution parameters for characterizing wind speeds. Renew. Energy **149**, 664–681 (2020)
4. Bouabdallah, S.: Design and control of quadrotors with application to autonomous flying. Technical Report (2007). https://doi.org/10.5075/epfl-thesis-3727
5. Bounemeur, A., Chemachema, M., Essounbouli, N.: Indirect adaptive fuzzy fault-tolerant tracking control for mimo nonlinear systems with actuator and sensor failures. ISA Trans. **79**, 45–61 (2018)
6. Bouzid, Y., Siguerdidjane, H., Bestaoui, Y.: Flight control boosters for three-dimensional trajectory tracking of quadrotor: theory and experiment. Proc. Inst. Mech. Eng. Part I: J. Syst. Control Eng. **232**(6), 709–727 (2018)
7. Chiou, J.S., Tran, H.K., Shieh, M.Y., Nguyen, T.N.: Particle swarm optimization algorithm reinforced fuzzy proportional–integral–derivative for a quadrotor attitude control. Adv. Mech. Eng. **8**(9), 1687814016668705 (2016)
8. Fliess, M., Join, C.: Model-free control. Int. J. Control **86**(12), 2228–2252 (2013)
9. Fliess, M., Join, C.: Stability margins and model-free control: a first look. In: 2014 European Control Conference (ECC), pp. 454–459. IEEE, New York (2014)
10. Glida, H.E., Abdou, L., Chelihi, A.: Optimal fuzzy adaptive backstepping controller for attitude control of a quadrotor helicopter. In: 2019 International Conference on Control, Automation and Diagnosis (ICCAD), pp. 1–6 (2019). https://doi.org/10.1109/ICCAD46983.2019.9037915
11. Han, F., Jiang, J., Ling, Q.H., Su, B.Y.: A survey on metaheuristic optimization for random single-hidden layer feedforward neural network. Neurocomputing **335**, 261–273 (2019)
12. Hasseni, S.E.I., Abdou, L.: Decentralized pid control by using GA optimization applied to a quadrotor. J. Autom. Mobile Robot. Intell. Syst. **12**, 33–44 (2018)
13. Hasseni, S.E.I., Abdou, L., Glida, H.E.: Parameters tuning of a quadrotor PID controllers by using nature-inspired algorithms. Evol. Intell. (2019). https://doi.org/10.1007/s12065-019-00312-8
14. Jia, Z., Yu, J., Mei, Y., Chen, Y., Shen, Y., Ai, X.: Integral backstepping sliding mode control for quadrotor helicopter under external uncertain disturbances. Aerosp. Sci. Technol. **68**, 299–307 (2017)
15. Jiang, X.Y., Su, C.L., Xu, Y.P., Liu, K., Shi, H.Y., Li, P.: An adaptive backstepping sliding mode method for flight attitude of quadrotor UAVs. J. Central South Univ. **25**(3), 616–631 (2018)
16. JiGuang, L., Xin, C.: A robust enhancement system based on observer-backstepping controller. J. Vis. Commun. Image Represent. **57**, 34–38 (2018)
17. Labbadi, M., Cherkaoui, M.: Robust adaptive backstepping fast terminal sliding mode controller for uncertain quadrotor UAV. Aerosp. Sci. Technol. **93**, 105306 (2019)
18. Laha, D., Gupta, J.N.: An improved cuckoo search algorithm for scheduling jobs on identical parallel machines. Comput. Ind. Eng. **126**, 348–360 (2018)
19. Li, C., Zhang, Y., Li, P.: Full control of a quadrotor using parameter-scheduled backstepping method: implementation and experimental tests. Nonlinear Dyn. **89**(2), 1259–1278 (2017)
20. Li, Z., Ma, X., Li, Y.: Model-free control of a quadrotor using adaptive proportional derivative-sliding mode control and robust integral of the signum of the error. Int. J. Adv. Robot. Syst. **15**(5), 1729881418800885 (2018)
21. Li, Z., Ma, X., Li, Y.: Robust tracking control strategy for a quadrotor using RPD-SMC and RISE. Neurocomputing **331**, 312–322 (2019)
22. Lin, J.: Oppositional backtracking search optimization algorithm for parameter identification of hyperchaotic systems. Nonlinear Dyn. **80**(1–2), 209–219 (2015)
23. Liu, Y., Qi, N., Yao, W., Liu, Y., Li, Y.: Optimal scheduling for aerial recovery of multiple unmanned aerial vehicles using genetic algorithm. Proc. Inst. Mech. Eng. Part G: J. Aerosp. Eng. (2019). https://doi.org/10.1177/0954410019842487
24. Mareli, M., Twala, B.: An adaptive Cuckoo search algorithm for optimisation. Appl. Comput. Inf. **14**(2), 107–115 (2018)
25. Meng, W., Yang, Q., Jagannathan, S., Sun, Y.: Adaptive neural control of high-order uncertain nonaffine systems: a transformation to affine systems approach. Automatica **50**(5), 1473–1480 (2014)
26. Mohd Basri, M.A., Husain, A.R., Danapalasingam, K.A.: A hybrid optimal backstepping and adaptive fuzzy control for autonomous quadrotor helicopter with time-varying disturbance. Proc. Inst. Mech. Eng. Part G: J. Aerosp. Eng. **229**(12), 2178–2195 (2015)
27. Mohd Basri, M.A., Husain, A.R., Danapalasingam, K.A.: Intelligent adaptive backstepping control for mimo uncertain non-linear quadrotor helicopter systems. Trans. Inst. Meas. Control **37**(3), 345–361 (2015)
28. Muñoz, F., González-Hernández, I., Salazar, S., Espinoza, E.S., Lozano, R.: Second order sliding mode controllers for altitude control of a quadrotor UAS: real-time implementation in outdoor environments. Neurocomputing **233**, 61–71 (2017)

29. Mustafa, G.I., Wang, H., Tian, Y.: Vibration control of an active vehicle suspension systems using optimized model-free fuzzy logic controller based on time delay estimation. Adv. Eng. Softw. **127**, 141–149 (2019)
30. Nadda, S., Swarup, A.: On adaptive sliding mode control for improved quadrotor tracking. J. Vib. Control **24**(14), 3219–3230 (2018)
31. Ouyang, F., Cheng, H., Lan, Y., Zhang, Y., Yin, X., Hu, J., Peng, X., Wang, G., Chen, S.: Automatic delivery and recovery system of wireless sensor networks (WSN) nodes based on UAV for agricultural applications. Comput. Electron. Agric. **162**(2), 31–43 (2019)
32. Özbek, N.S., Önkol, M., Efe, M.Ö.: Feedback control strategies for quadrotor-type aerial robots: a survey. Trans. Inst. Meas. Control **38**(5), 529–554 (2016)
33. Panomrattanarug, B., Higuchi, K., Mora-Camino, F.: Attitude control of a quadrotor aircraft using LQR state feedback controller with full order state observer. In: The SICE Annual Conference 2013, pp. 2041–2046. IEEE, New York (2013)
34. Premkumar, K., Manikandan, B.: Bat algorithm optimized fuzzy PD based speed controller for brushless direct current motor. Eng. Sci. Technol. Int. J. **19**(2), 818–840 (2016)
35. Priya, K., Rajasekar, N.: Application of flower pollination algorithm for enhanced proton exchange membrane fuel cell modelling. Int. J. Hydrog. Energy **44**, 18438–18449 (2019)
36. Qin, Y., Rath, J.J., Hu, C., Sentouh, C., Wang, R.: Adaptive nonlinear active suspension control based on a robust road classifier with a modified super-twisting algorithm. Nonlinear Dyn. **97**(4), 2425–2442 (2019)
37. Qiu, J., Sun, K., Rudas, I.J., Gao, H.: Command filter-based adaptive NN control for MIMO nonlinear systems with full-state constraints and actuator hysteresis. IEEE Trans. Cybern. (2019). https://doi.org/10.1109/TCYB.2019.2944761
38. Slotine, J.J.E., Li, W., et al.: Applied nonlinear control, vol. 199. Prentice hall, Englewood Cliffs, NJ (1991)
39. Talbi, N.: Design of fuzzy controller rule base using bat algorithm. Energy Proc. **162**, 241–250 (2019)
40. Wang, G.G., Chu, H.E., Mirjalili, S.: Three-dimensional path planning for UCAV using an improved bat algorithm. Aerosp. Sci. Technol. **49**, 231–238 (2016)
41. Woellner, R., Wagner, T.C.: Saving species, time and money: application of unmanned aerial vehicles (UAVs) for monitoring of an endangered alpine river specialist in a small nature reserve. Biol. Conserv. **233**, 162–175 (2019)
42. Yan, K., Chen, M., Wu, Q.: Neural network-based adaptive fault tolerant tracking control for unmanned autonomous helicopters with prescribed performance. Proc. Inst. Mech. Eng. Part G: J. Aerosp. Eng. **233**(12), 4350–4362 (2019)
43. Zeghlache, S., Kara, K., Saigaa, D.: Fault tolerant control based on interval type-2 fuzzy sliding mode controller for coaxial trirotor aircraft. ISA Trans. **59**, 215–231 (2015)
44. Zhang, J., Ren, Z., Deng, C., Wen, B.: Adaptive fuzzy global sliding mode control for trajectory tracking of quadrotor UAVs. Nonlinear Dyn. **97**, 1–19 (2019)
45. Zhang, R., Jiang, X., Li, R.: Improved decomposition-based multi-objective Cuckoo search algorithm for spectrum allocation in cognitive vehicular network. Phys. Commun. **34**, 301–309 (2019)
46. Zhang, X., Lu, X., Jia, S., Li, X.: A novel phase angle-encoded fruit fly optimization algorithm with mutation adaptation mechanism applied to UAV path planning. Appl. Soft Comput. **70**, 371–388 (2018)
47. Zhao, L., Dai, L., Xia, Y., Li, P.: Attitude control for quadrotors subjected to wind disturbances via active disturbance rejection control and integral sliding mode control. Mech. Syst. Signal Process. **129**, 531–545 (2019)
48. Zhen, Z., Xing, D., Gao, C.: Cooperative search-attack mission planning for multi-UAV based on intelligent self-organized algorithm. Aerosp. Sci. Technol. **76**, 402–411 (2018)
49. Zhou, Y., Miao, F., Luo, Q.: Symbiotic organisms search algorithm for optimal evolutionary controller tuning of fractional fuzzy controllers. Appl. Soft Comput. **77**, 497–508 (2019)
50. Zhu, Y., Zheng, W.X.: Multiple Lyapunov functions analysis approach for discrete-time switched piecewise-affine systems under dwell-time constraints. IEEE Trans. Autom. Control (2019). https://doi.org/10.1109/TAC.2018.2797173
51. Zhu, Y., Zhong, Z., Basin, M.V., Zhou, D.: A descriptor system approach to stability and stabilization of discrete-time switched PWA systems. IEEE Trans. Autom. Control **63**(10), 3456–3463 (2018). https://doi.org/10.1109/TAC.2019.2938302